

# Effects of ball milling on pure antimony, on Ga-Sb alloy and on Ga + Sb powder mixture; oxidation, glass formation and crystallization

## A. Tonejc

Faculty of Science, Department of Physics, P.O. Box 162, 41000 Zagreb, and Institute of Physics University of Zagreb, P.O. Box 304, 41001 Zagreb (Yugoslavia)

## D. Dužević

Rade Končar Elektrotechnical Institute, Baštijanova bb, 41000 Zagreb (Yugoslavia)

## A. M. Tonejc

Faculty of Science, Department of Physics, P.O. Box 162, 41000 Zagreb, and Institute of Physics University of Zagreb, P.O. Box 304, 41001 Zagreb (Yugoslavia)

### Abstract

Elemental polycrystalline antimony powder, a mixture of antimony and gallium powder, and a Ga-88at.%Sb alloy were mechanically alloyed or ground by high-energy ball milling in an air atmosphere. An excessive oxidation of antimony was observed and this gave us the possibility to estimate the temperature of the milling process in our case. The mechanical grinding of the Ga-88at.%Sb alloy first produced an amorphous oxide, which subsequently crystallized on further milling.

## 1. Introduction

Since Koch *et al.* [1] and Ermakov *et al.* [2] showed that amorphous alloy powders can be produced by the mechanical alloying (MA) of a mixture of elemental powders [1] or by mechanical grinding (MG) of the compounds [2], the MA and MG techniques have been applied extensively to many systems, increasingly replacing the liquid quenching (LQ) and vapour quenching (VQ) techniques, although they are still the usual ways to prepare non-equilibrium materials.

Antimony has an equilibrium rhombohedral structure, but in antimony foils, prepared by LQ, some metastable structures have been observed [3]. Antimony films prepared by VQ show the same metastable phases if deposited on substrates held at room temperature and an amorphous structure when deposited at liquid air temperature [3]. Applying LQ to the Ga-88at.%Sb alloy, a metastable solubility of gallium in antimony of about 3.5 at.% was obtained [4]. (The phase diagram of Ga-Sb shows no solid solubility of gallium in antimony [5].)

Since the MA and MG techniques have shown,

in some cases, to be even more efficient in producing amorphous materials in comparison to LQ (*e.g.* [6, 7]), we decided to apply both techniques on pure antimony, on a mixture of elemental powders of antimony and gallium (at 88/12 atomic proportion), and on a Ga-88at.%Sb alloy.

## 2. Experimental procedure

Elemental antimony and gallium powders were mixed to obtain the desired average composition, then placed in an agate vial together with 12 hard-metal balls and subsequently ball milled in air. The total mass of powder was about 2.5 g. Further experimental details of ball milling have been reported earlier [8]. The Ga-88at.%Sb ingots were prepared by means of direct synthesis [4], then broken into small pieces and subjected to ball milling (MG treatment) in the same manner as that used for elemental powders.

The milling was performed at room temperature, and at selected times the milling process was interrupted, small quantities of powder were

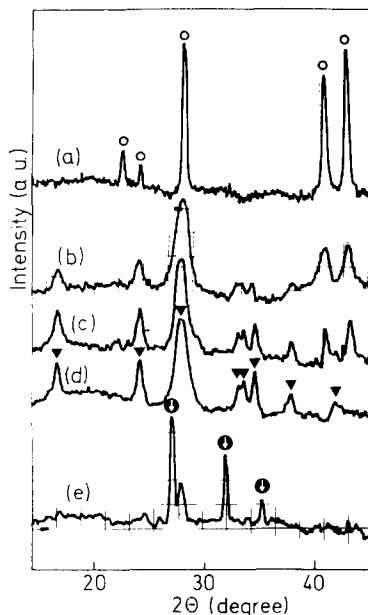


Fig. 1. X-ray diffraction patterns for antimony treated by MG: (a) before milling; (b) after 2 h milling; (c) after 12 h milling; (d) after 16 h milling; (e) powders of (d) annealed in vacuum at 410 °C for 4.5 h. ○: rhombohedral antimony; ▼: high-temperature orthorhombic  $\text{Sb}_2\text{O}_3$ ; ●: low-temperature f.c.c.  $\text{Sb}_2\text{O}_3$ .

removed and subjected to X-ray investigation. The X-ray diffraction patterns were obtained using  $\text{CuK}\alpha$  radiation and a Nonius Guinier-de Wolff quadruple focusing camera.

### 3. Results

#### 3.1. Ball milling of elemental antimony

Figures 1(a)–1(d) show a series of X-ray diffraction patterns obtained at various time intervals during the ball milling of elemental antimony powder. After 2 h of processing (Fig. 1(b)), a decrease in intensity of antimony Bragg peaks and the appearance of some new Bragg peaks were observed. On further ball milling the new Bragg peaks were gaining intensity (Fig. 1(c)), while the antimony peaks were decreasing, and disappeared after 16 h of processing (Fig. 1(d)). The diffraction patterns of the new crystalline phase did not change on further milling for up to 48 h. The new phase was identified as the high-temperature orthorhombic  $\text{Sb}_2\text{O}_3$  phase [9].

#### 3.2. MA of a mixture of elemental antimony and gallium

The MA of the mixture of elemental powders of antimony and gallium at 88/12 atomic propor-

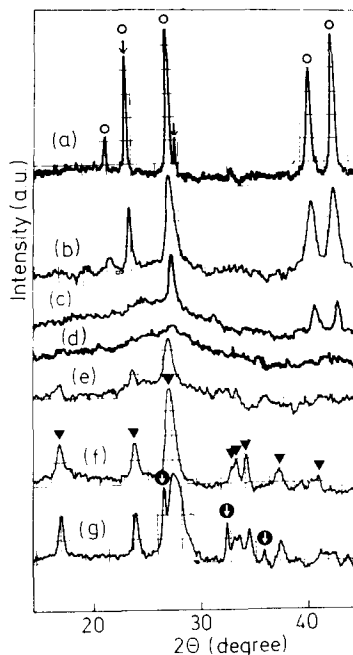


Fig. 2. X-ray diffraction patterns for Sb-88at.%Ga alloy treated by MG: (a) before milling; (b) after 2 h milling; (c) after 12 h milling; (d) after 16 h milling; (e) after 24 h milling; (f) after 52 h milling; (g) powders of (d) annealed in vacuum at 410 °C for 5 days. ▲: cubic GaSb; ○: rhombohedral antimony; ▼: high-temperature orthorhombic  $\text{Sb}_2\text{O}_3$ ; ●: low-temperature f.c.c.  $\text{Sb}_2\text{O}_3$ .

tion showed that there was virtually no difference in the diffraction patterns obtained for pure antimony and for the powder mixture. The quantity of gallium powder was obviously too small to be detected on the diffraction patterns. After 16 h of milling the  $\text{Sb}_2\text{O}_3$  phase was the only phase detected, while the diffraction patterns showed no changes with further milling.

#### 3.3. MG of Ga-88at.%Sb compound

The diffraction patterns showed that the peaks belonging to the cubic GaSb intermetallic phase gradually disappeared with MG, and the antimony lines showed some broadening (Figs. 2(a)–2(b)). After 8 h of MG the GaSb peak was no longer present and, with further grinding, the peaks of antimony began gradually to disappear without showing further line broadening, while a broad diffuse diffraction maximum was growing separately (Fig. 2(c)). After 16 h of MG only this broad diffraction maximum was visible on the diffraction patterns (Fig. 2(d)), indicating the presence of the amorphous structure.

When the grinding was continued beyond the complete amorphization, the amorphous phase

began to crystallize (Fig. 2(e)) and the powder was again completely crystalline after 52 h of total milling (Fig. 2(f)). The crystalline phase was the high-temperature  $\text{Sb}_2\text{O}_3$ , the X-ray patterns of which showed no changes with further MG.

### 3.4. Annealing

Certain powders, after ball milling, were heat treated in evacuated quartz capillary tubes to make possible a better explanation of the obtained milling products.

When the powders of high-temperature  $\text{Sb}_2\text{O}_3$  phase obtained by the MG and MA processes were annealed at 610 °C, the diffraction lines became sharper, but no new Bragg lines were detected. However, when annealed at a temperature of 410 °C for only 4.5 h, the high-temperature orthorhombic  $\text{Sb}_2\text{O}_3$  phase almost completely transformed into the low-temperature  $\text{Sb}_2\text{O}_3$  phase (Fig. 1(e)), which is of the cubic structure [9].

However, amorphous powders showed to be more stable against the transformation. Annealing for 4.5 h at 410 °C showed no change in the diffraction pattern, but after 5 days the diffraction patterns showed both the low-temperature and high-temperature  $\text{Sb}_2\text{O}_3$  phase (Fig. 2(g)).

## 4. Discussion

### 4.1. Ball-milling temperature

Past experiments performed on Cu–Nb–Sn alloys have shown that even when the ball milling was performed in air, no extra diffraction peaks corresponding to oxides were seen on the X-ray diffraction patterns after 24 h of milling [10]. This was why we found the excessive oxidation of antimony powder in our ball-milling experiments rather unusual. However, the oxidation process helped us to estimate the local peak temperatures that appeared during the ball-milling process.

Many authors agree that powder particles trapped between colliding balls are subjected to frictional glide and plastic deformation which locally heats the powder particles, but there is disagreement regarding the value of the respective temperature (higher than melting point [2], above crystallization temperature [11], of the order of the crystallization temperature [12]). However, these estimations are in contradiction with the calculations of Schwartz and Koch [13] who claimed that the temperature rise during MA does not exceed 38 K.

The orthorhombic high-temperature  $\text{Sb}_2\text{O}_3$  phase which appeared in our milling process is stable at temperatures above 570 °C, and below 570 °C it transforms to low-temperature cubic  $\text{Sb}_2\text{O}_3$  [9], a fact confirmed by our annealing experiments. From the results we obtained in ball-milling and annealing processes it is clear that the local increase of temperature in the milling process was rather high, at least of the order of the crystallization temperature of the amorphous oxide. This is in agreement with the results obtained by Trudeau *et al.* [12].

Since the temperature of the outer walls of the agate vial never exceeds 50 °C, no matter how long the duration of uninterrupted milling experiment, it is further evidence that the increase of temperature is really of a local nature.

### 4.2. MA and MG treatment of Ga–88at.%Sb powder mixtures

The MA of antimony and gallium powder mixtures (proportion 88/12) and the MG of the Ga–88at.%Sb alloy showed that the high-temperature crystalline form of  $\text{Sb}_2\text{O}_3$  began to form in the MA process, and the amorphous phase in the case of MG. Since no gallium or gallium-oxide lines were detected on X-ray patterns, we assume that either gallium evaporated in the initial stages of MG and MA, or it oxidized forming a  $(\text{Sb}_{2-x}\text{Ga}_x)\text{O}_3$ . However, further investigations are needed to clarify this point.

After approximately 16 h only the crystalline  $\text{Sb}_2\text{O}_3$  was present in the MA procedure and only the amorphous phase in the MG procedure. However, on further MA and MG, the crystalline  $\text{Sb}_2\text{O}_3$  phase remained unchanged, but the amorphous phase began to crystallize into high-temperature  $\text{Sb}_2\text{O}_3$  form.

The vacuum annealing experiments of the amorphous phase that we have carried out at temperatures well below the transformation temperature “high-temperature  $\text{Sb}_2\text{O}_3$  → low-temperature  $\text{Sb}_2\text{O}_3$ ”, have revealed that both oxides appear simultaneously on diffraction patterns.

It is not clear at this stage of investigations which factor is responsible for the fact that in MA procedure the crystalline high-temperature  $\text{Sb}_2\text{O}_3$  is formed directly, while in the MG procedure, first the amorphous oxide is formed which, with prolonged milling, transforms to crystalline  $\text{Sb}_2\text{O}_3$ .

## 5. Conclusions

We observed excessive oxidation of antimony in the ball-milling procedure in air. A high-temperature  $\text{Sb}_2\text{O}_3$  phase was formed which allowed us to conclude that the local temperature in the ball-milling process was of the order of the crystallization temperature of the amorphous phase.

In the MA process the  $\text{Sb}_2\text{O}_3$  oxide appeared in crystalline form, but in the MG procedure we first observed an oxide glass formation which crystallized on further milling. The amorphous oxide remained quite stable at temperatures below 410 °C, and no crystallization process was detected after 5 h of annealing at 410 °C; but after annealing at this temperature for 5 days, both high-temperature and low-temperature crystalline oxide forms appeared on the diffraction patterns.

## References

- 1 C. C. Koch, O. B. Cavin, C. G. McKamey and J. O. Scarbrough, *Appl. Phys. Lett.*, *43* (1983) 1017.
- 2 A. E. Ermakov, E. E. Yurchikov and V. A. Barinov, *Fiz. Met. Metalloved.*, *52* (1981) 1184.
- 3 D. Akhtar, V. D. Vankar, T. C. Goel and K. L. Chopra, *J. Mater. Sci.*, *14* (1979) 988.
- 4 A. Bonefačić, A. Tonejc and Z. Ogorelec, *Scr. Metall.*, *23* (1989) 1212.
- 5 M. Hansen and K. Anderko (eds.), *Constitution of Binary Alloys*, 2nd edn., McGraw-Hill Book Co., New York, 1958, p. 755.
- 6 L. Schultz, *Mater. Sci. Eng.*, *97* (1988) 15.
- 7 K. F. Kobayashi, N. Tachibana and P. H. Shingu, *J. Mater. Sci.*, *25* (1990) 801.
- 8 M. Stubičar and D. Dužević, in W. A. Kaysser and J. Weber-Bock (eds.), *Emerging Materials by Advanced Processing*, KFA Jülich, 1989, pp. 237–250.
- 9 R. P. Elliot, *Constitution of Binary Alloys*, First Supplement, McGraw-Hill Book Company, London, 1965, p. 691.
- 10 A. Inoue, H. K. Kimura, K. Matsuki and T. Masumoto, *J. Mater. Sci. Lett.*, *6* (1987) 979.
- 11 J. Eckert, L. Schultz, E. Hellstern and K. Urban, *J. Appl. Phys.*, *64* (1988) 3224.
- 12 M. L. Trudeau, R. Schultz, D. Dussault and A. Van Neste, *Phys. Rev. Lett.*, *64* (1990) 99.
- 13 R. B. Schwartz and C. Koch, *Appl. Phys. Lett.*, *49* (1986) 146.